AEDC-TR-71-265

EVALUATION OF PROBES FOR MEASURING STATIC PRESSURE IN SUPERSONIC AND HYPERSONIC FLOWS

J. Don Gray

ARO, Inc.

January 1972

VON KÁRMÁN GAS DYNAMICS FACILITY
ARNOLD ENGINEERING DEVELOPMENT CENTER
AIR FORCE SYSTEMS COMMAND
ARNOLD AIR FORCE STATION, TENNESSEE

NOTICES

When U. S. Government drawings specifications, or other data are used for any purpose other than a definitely related Government procurement operation, the Government thereby incurs no responsibility nor any obligation whatsoever, and the fact that the Government may have formulated, furnished, or in any way supplied the said drawings, specifications, or other data, is not to be regarded by implication or otherwise, or in any manner licensing the holder or any other person or corporation, or conveying any rights or permission to manufacture, use, or sell any patented invention that may in any way be related thereto.

Qualified users may obtain copies of this report from the Defense Documentation Center.

References to named commercial products in this report are not to be considered in any sense as an endorsement of the product by the United States Air Force or the Government.

EVALUATION OF PROBES FOR MEASURING STATIC PRESSURE IN SUPERSONIC AND HYPERSONIC FLOWS

J. Don Gray
ARO, Inc.

FOREWORD

This report summarizes work sponsored by the Arnold Engineering Development Center (AEDC), Air Force Systems Command (AFSC), Arnold Air Force Station, Tennessee, under Program Element 62201F, Project 8219.

The work reported herein was done by ARO, Inc. (a subsidiary of Sverdrup & Parcel and Associates, Inc.), contract operator of the AEDC, AFSC, under Contract F40600-C-72-0003. These results were organized during the period from July to October, 1970, under ARO Project VT0036, and the manuscript was submitted for publication on November 3, 1971.

This technical report has been reviewed and is approved.

Emmett A. Niblack, Jr.
Lt Colonel. USAF
AF Representative, VKF
Directorate of Test

Duncan W. Rabey, Jr.
Colonel, USAF
Director of Test

ABSTRACT

The pertinent facts in the literature have been examined regarding the aerodynamic characteristics of static-pressure measuring probes in order to assess the relative merits and limitations of cone-cylinder, sharp-cone, and planar (disk) probes. The effects of Mach number, angle of attack, orifice location, and Reynolds number on the inferred local pressures were all evaluated at Mach numbers up to 8. It is concluded that the planar probe and sharp-cone probe (if properly designed) are equally more accurate than the cone-cylinder probe at supersonic and hypersonic speeds. However, the cone-cylinder is judged to be superior for use at Mach numbers below 4. Details of a recommended procedure to correct for the effects of viscous interaction (all probes) and angle of attack (planar probes only) are included.

CONTENTS

Page

ABSTRACT iii
NOMENCLATURE vi
I. INTRODUCTION 1
II. DISCUSSION OF PROBE CHARACTERISTICS
2.1 Axisymmetric Probes 1
2.2 Planar Probes 5
III. CONCLUSIONS 6
REFERENCES 8

APPENDIXES

I. ILLUSTRATIONS

Figure

1. Typical Effect of Mach Number on the Longitudinal Surface Pressure Distribution on a Slender Cone-Cylinder Model at $\alpha = 0$ 13
2. Effects of Mach Number and Angle of Attack on the Circumferential Pressure Variation of a Slender Cone-Cylinder at X/D = 13 14
3. Effects of Mach Number and Circumferential Location on the Pressure Ratio Variation with Angle of Attack for a Cone-Cylinder at X/D = 13 15
4. Influence of Mach Number on the Maximum Sensitivity of Cylinder Pressure Ratio to Angle-of-Attack Variation, $\omega = 0$ 16
5. Circumferential Pressure Distributions for Cylinders Normal to Flow, Experimental Results 17
6. Comparison of Yawed Cone-Cylinder Circumferential Pressures with Transformed Distributions of Cylinders in Normal Flow 18
7. Effects of Mach Number on Circumferential Cylinder Pressures at $\alpha = 10$ deg Predicted by the Transformation of Normal Flow Data 19
8. Effects of Mach Number on the Circumferential Pressure Variation of a 10-deg (Semiangle) Cone at $\alpha = 10$ deg 20
9. Effect of Cone Semiangle on the Circumferential Pressure Variation at $M_\infty = 8$ and $\alpha = 10$ deg 22
10. Effect of Angle of Attack on Cone Pressures 23
11. Influence of Roll Orientation on Averages of Cone Pressure at 10-deg Yaw ($M_\infty = 8$ and $\theta_c = 12.5$ deg) 25
12. Effects of Mach Number and Cone Angle on the Pressure Increment Measured at $\alpha = 10$ deg 26
13. Influence of Mach Number on the Maximum Sensitivity of Flat-Plate Pressure to an Angle of Attack, Inviscid Flow 27
14. Effects of Mach Number on the Influence of Nose Bluntness on Inviscid Pressures on a Flat Plate, $\alpha = 0$ 28
15. Example of the Applicability of Flat-Plate Measurements in Multiple Shock Flows Using Single Shock Calibration Curve, a Theoretical Analysis 29

Page

II. WEAK-INTERACTION AND ALIGNMENT CORRECTION PROCEDURE . . . 31

III. PROCEDURE FOR EVALUATING THE PLATE ALIGNMENT FACTOR . . . 34

NOMENCLATURE

C	Chapman-Rubesin viscosity parameter, $(\mu_w/\mu)(T/T_w)$
D	Reference diameter of cylinder, in.
ℓ	Surface length to orifice, in.
M	Mach number
P	Pressure coefficient, $(p_w - p_\infty)/q_\infty$
p	Static pressure, psia
$p_c(a)$	Cone surface pressure at a, psia
$\bar{p}_c(a)$	Average cone surface pressure at a, psia
p_p	Pitot pressure, psia
q	Dynamic pressure, $\gamma pM^2/2$, psia
R_N	Nose radius, in.
Re_D	Free-stream Reynolds number based on D
Re_ℓ	Reynolds number based on length ℓ
X	Axial distance from nose, in.
T	Temperature, °R
a	Angle of attack, deg
γ	Ratio of specific heats for air, 1.40
θ_c	Cone semiangle, deg
μ	Absolute viscosity, lb_f-sec/ft^2
ϕ	Roll angle, deg

$\bar{\chi}$ Viscous interaction parameter, $M^3/\sqrt{Re_\ell/C}$

ω Circumferential angle around body, measured from the windward generator, deg

SUBSCRIPTS

∞ Free stream

i Inviscid

t Total

w Wall or surface value

SECTION I
INTRODUCTION

The determination of local static pressure is generally acknowledged to be considerably more difficult at supersonic speeds than it is in subsonic or transonic flows. As a consequence it is a measurement seldom attempted, and when it is, any inconsistencies with surface data produce suspicion of all such data obtained. This situation is unfortunate since it exists primarily because of a lack of organized information concerning (1) the influence of the relevant aerodynamic parameters and (2) the limitations of conventional techniques for measuring flow-field static pressure. It is the purpose of this report to collect and examine the pertinent facts on this subject.

The methods considered to be conventional are all based on the measurement of the surface pressure(s) on either planar or axisymmetric bodies of small size. The small size, of course, is dictated by the needs (1) to make measurements close to a wall or between the surface and bow wave and (2) to minimize the effects of local static-pressure gradients. Planar probes are sharp-leading-edge flat plates of either rectangular (flat-plate) or circular (disk) planform. Flat-plate probes have been used in sonic boom studies to measure pressure field signatures, whereas disk probes have been used more generally (e.g., Refs. 1 and 2). Axisymmetric probes are either cylinders with sharp noses or sharp-tipped slender cones. The cone-cylinder probe (Ref. 3), or variations of it (Ref. 4), has received the widest acceptance of all methods, most likely because of its small diameter. The use of a small cone probe (Ref. 5) to determine local static pressure differs fundamentally from the other methods in that it requires knowledge of the relationship between the measured pressure on the cone and that in the local free stream.

In principle, a location on all probes (other than the cone probe) can be chosen such that the inviscid measurement of the local static pressure is direct and independent of Mach number, whereas every probe is fundamentally sensitive to flow angularity and/or misalignment effects. In addition to this error introduced by angle of attack or yaw, corrections are required to account for viscous effects manifest as (1) self-induced pressure gradients on the probe and as (2) shock wave boundary-layer interactions when the probe traverses severe flow-field pressure gradients.

SECTION II
DISCUSSION OF PROBE CHARACTERISTICS

2.1 AXISYMMETRIC PROBES

2.1.1 Cone-Cylinder Configuration

Typical longitudinal surface pressure variations with free-stream Mach number ($1.75 \leq M_\infty \leq 4.5$) are presented for a slender, cone-cylinder configuration in Fig. 1, Appendix I. These data (from Ref. 6) show that the surface pressure must be measured far downstream of the shoulder (at least 8D) to be a close approximation of the free-stream pressure. These data also indicate that the pressure ratio, p/p_∞, at a fixed station decreases with Mach number increase. It is interesting to note the influence which nose shape has

on these effects. Transonic data and hypersonic data ($M_\infty \leq 8$) for hemispherical noses (Ref. 7) show that nose shape influences on the cylinder pressure are not discernible at distances of 8D from the shoulder. This observation is generally supported in Ref. 8 by data for $M_\infty = 7.5$; but, because of viscous effects, it was recommended that the measurement station be at least twice as far from the shoulder (16D). Thus nose shape is not a critical requirement in the design of a "cone-cylinder" probe.

Typical circumferential surface pressure variations on a slender, cone-cylinder configuration are presented in Fig. 2 to show the effects of Mach number and angle of attack. The significant point illustrated by these data is that the location of the measured pressure equal to the free-stream value varied from about 30 to 50 deg (relative to the windward generator) moving toward the 90-deg location–the hypersonic, Newtonian limit as Mach number increases. This sensitivity of measurement to angle-of-attack variation is shown in Fig. 3 for the above noted extremes, since the location $\omega \approx 40$ deg is approximately the minimum value recommended in Ref. 9, and the $\omega = 90$ deg location is the location most often observed in actual use. It is obvious from this figure that the 90-deg location is not best, but that the $\omega \approx 40$ deg position in the range $1.75 \leq M_\infty \leq 4.5$ and $-2 \text{ deg} < \alpha \leq 6$ deg will measure a pressure within ±5 percent of the free-stream value. The maximum effect of angle of attack, of course, is measured on the windward generator ($\omega = 0$), and the fact that it can be reasonably well estimated by impact (Newtonian) theory is demonstrated in Fig. 4. The basic data in Fig. 4a (from Ref. 6) have been replotted in Fig. 4b versus the appropriate Newtonian parameter to show that a good correlation exists and that the error caused by any misalignment grows as $(M \sin \alpha)^2$.

Since the data of Ref. 6) were limited to $M_\infty \leq 4.5$, it is quite uncertain whether the ideal circumferential measurement position moves closer to $\omega = 90$ deg at much higher Mach numbers. In order to examine this question further the sweepback principle of Ref. 10 is invoked. This principle concerns the independence of viscous flow in planes normal to the axis of a cylinder from the flow in planes parallel to the axis. Thus it is possible to relate the flow over long cylinders at different free-stream conditions and angles of attack solely by the component of velocity in planes at right angles to the cylindrical axis. Utilizing pressure data (Refs. 11 and 12) obtained on cylinders normal to the flow (see Fig. 5) the principle was applied to the conditions corresponding to the data of Fig. 2 with the results shown in Fig. 6. Because of this excellent agreement, the substantial predicted effect of Mach number shown in Fig. 7 must be considered representative. Hence, in the range from $0 \leq M \leq 10$ (see small inset curve at top of Fig. 7) the circumferential position of the pressure equal to free-stream value is predicted to move over an increment of 40 deg. Consequently, it is not possible to design a static-pressure probe insensitive to flow angularity effects for surveying hypersonic flow fields. However, these results do indicate that a probe fairly insensitive to flow angularity (from one direction) can be designed for Mach numbers up to about four. It is suggested that if precise static-pressure measurements are required in flow fields of large streamline curvature, it would be necessary to measure (1) the differential pressures with a flow angularity probe and (2) the Mach number with a pitot probe. Then by an iteration procedure the effects of Mach number and angularity on the static-pressure measurement could be corrected using the sweepback principle to deduce the free-stream value.

In continuum flow, the effects of Reynolds number on the displacement thickness-induced pressure perturbation on a cone-cylinder apparently has been examined only in Refs. 8, 13, and 14. In Ref. 8 it was shown, at least for $6 \leq M_\infty \leq 7.5$, that the viscous-induced pressure increments at various axial hole locations could not be correlated by the interaction parameter, $\bar{\chi}$. It was shown, however, that at each location the induced pressure was linearly dependent on $\bar{\chi}$ being the least sensitive at the most aft location (about 13D from the shoulder). Williams (Ref. 8) concluded it must be presumed that a residual dependence on Mach number exists for this interaction. In the absence of further data it is recommended that these results be used in the form

$$p_w/p = 1 + [0.212 - 0.01\ \Delta X/D]\ \bar{\chi}$$

where ΔX = distance between shoulder and orifice, measured in inches.

It may be noted that this expression reduces to $p_w/p = 1 + 0.132\ \bar{\chi}$ when $\Delta X/D = 8$, and that this coefficient of $\bar{\chi}$ is much less than the theoretical flat-plate value (which is indicated in Ref. 15 to be 0.31, to first order). It is to be noted also that even for low density flows a linear correlation of p_w/p with $\bar{\chi}$ has been observed (Ref. 16).

Viscous interactions induced by shock waves are readily obtained during surveys through severe adverse static-pressure gradient regions as well as through shock waves. The effect is manifest just like the pressure distribution on a flat plate with an impinging shock (see Fig. 5 of Ref. 3), but the effect can be almost entirely eliminated by tripping the boundary layer on the probe (Ref. 3) as long as the wave is not strong enough to separate a turbulent boundary layer. An additional shock-induced interaction of considerable importance is that produced where the probe is enlarged downstream to provide a rigid stem for attachment to some probe support. This flare can produce a significant interaction when the Reynolds number and/or the flare angle is large. A reasonable maximum value of 10 deg (semiangle) for this flare is suggested to minimize the interaction; since the data in Ref. 17 indicate that the size of the interaction at high Reynolds number could approach 40 percent of the wetted length to the flare, it is recommended that the distance from the orifice to the flare be the same as that from the shoulder to the orifice (i.e., at least 8D).

2.1.2 Sharp Cone Configuration

Characteristic effects of Mach number on the circumferential pressure distribution of a yawed sharp[1] cone are illustrated in Fig. 8 by the inviscid flow solutions of Ref. 18. In contrast to the yawed cylinder, it is particularly evident— in Fig. 8b— that the circumferential location of the pressure equal to the unyawed pressure is considerably less sensitive to Mach number. Since the inviscid surface pressure is constant along rays from the apex of the cone, the longitudinal location is unimportant; on the other hand, the local free-stream Mach number must be known in order to infer the local free-stream pressure from measurements on a cone. It can be seen in Fig. 9 that the circumferential

[1]All subsequent discussion concerns only cones which are sharp aerodynamically.

rate of change of pressure varies inversely with cone angle, whereas the free-stream pressure location is hardly affected. As a result of this trend, the circumferential variation becomes more regular tending toward the Newtonian (sin ω) dependence. The effect of angle of attack on the circumferential pressure variation is shown in Fig. 10a to be generally the same as that shown for cone angle. A hypersonic correlation of inviscid results for $\alpha \leq 10$ deg, presented in Fig. 10b, shows that the maximum increment in pressure relative to free stream is well correlated using a coordinate derived from Newtonian impact theory, but that the perturbation caused by angle of attack grows in a less direct manner than that shown in Fig. 4b for planar probes. In order to minimize the effects of flow angle, an average of pressures measured at different circumferential positions has been used (Ref. 19). Inviscid pressures 90 deg apart (four positions) and 180 deg apart (two positions) were averaged over a 180-deg range of roll variation in order to illustrate (see Fig. 11) the decreased sensitivity of these mean pressures to angle of attack. It is noted that four pressures averaged are much less sensitive to the roll orientation than two pressures, and that the relative variation is much smaller with respect to the unyawed cone pressure (Fig. 11a) than it is with respect to the free-stream pressure (Fig. 11b). Of course with the four pressures individually measured it is possible (if pitot pressure is known) to correct for yaw using the procedure outlined in Ref. 19. The problem with this approach is the size limitation imposed by four tubes installed in a small probe, especially small angle cones. It can be shown that a sensitivity parameter[2], $\cdot \partial(p_c/p_p)/\partial M_\infty \div (p_c/p_p)$ (at zero yaw), is the largest when the cone angle is the smallest. As a result very slender cones will yield the best definition of local free-stream Mach number. It is therefore apparent that some compromise between sensitivity and flow angularity effects is necessary. Because measurements are seldom required in a flow field for which there is more than one principal plane of streamline curvature or for which the general orientation of the plane is not known, it is feasible to make the measurements with two manifolded orifices oriented in the plane normal to the plane of flow inclination (i.e., ω = 90 deg). The results of an inviscid evaluation of this measurement position, presented in Fig. 12, indicate that the slenderest cone will yield the smallest pressure increment for a given angle of attack over the Mach number range of interest.

The effect of Reynolds number on the cone probe is extremely important because of its short length (compared to a cone-cylinder probe). Self-induced pressures caused by the displacement thickness growth on small (D = 1/4 in.) 12.5-deg cones have been measured (for example, Ref. 5) and found to be in fair agreement with weak-interaction theory corrected for conical flow. It is therefore suggested that the inviscid cone pressure be inferred from the measured value using the theoretical (Ref. 20) expression, $p_w/p_{iw} = 1 + 0.14\ \bar{\chi}_{iw}$. It is to be noted that this expression requires knowledge of the local inviscid Reynolds number and Mach number adjacent to the cone surface. Thus pitot pressure measurements are required, in addition to the appropriate inviscid cone solutions, so that the local free-stream pressure may be inferred after an iteration process to determine the weak-interaction correction. The general procedure to be followed is detailed in Appendix II. Comments made regarding the shock wave, boundary-layer interaction effects

[2]This parameter results when the error propagation of M_∞ is evaluated as $M_\infty = M_\infty(p_c, p_p)$ in terms of the relative errors of these basic measurements.

on the cone-cylinder apply in general to the cone probe. It should be noted that, for the same diameter, the Reynolds number on a cone may be up to one-sixth that on a cone-cylinder probe. This will reduce the scale of the shock interaction effects considerably, but it will also make it quite difficult to trip the boundary layer and eliminate the effects altogether.

A final point regarding this probe concerns its range of applicability. It cannot be used at subsonic and transonic speeds because of the absence of inviscid flow solutions.

2.2 PLANAR PROBES

The primary distinction between flat-plate and disk probes is in the planform, although the orientation of the plane relative to the plane of flow inclination is a distinction to be noted between them in practice. For example, in a previous investigation the flat-plate probe was orthogonal to the flow inclination plane, whereas in a subsequent test the disk probe was used parallel to the flow inclination plane. An inherent assumption in the use of a disk probe in supersonic flow is that the flow is identical to that for an infinite span flat plate. For the small angles of attack of interest here, this is a reasonable assumption. Hence, the subsequent discussion will be about disk probes in general.

The maximum inviscid pressure ratio variation with angle of attack (or yaw) is that predicted for an isentropic compression (or oblique shock compression for the conditions of interest here). This theoretical variation, presented in Fig. 13, shows quite clearly that the major problem in using a disk or plate probe is the alignment. For example, note that at $M_\infty = 8$ a 10 percent "error" would be produced by a misalignment of less than 0.5 deg. It is shown by the hypersonic approximation presented in Fig. 13a that the pressure perturbation (error) above free-stream level is directly proportional to both the angular misalignment and the local free-stream Mach number. Thus the ratio of the pressure perturbation for a disk relative to that for a cylinder varies approximately as $(M_\infty \sin \alpha)^{-1}$, utilizing this approximation and that previously shown in Fig. 4b.

Another important inviscid effect, which is more pronounced because of the two-dimensional flow, is the influence of the leading-edge radius which produces the blast wave effect on the pressure distribution. Results of inviscid calculations, presented next in Fig. 14, show, for example, at $M_\infty = 6$ that with a leading-edge radius of $R_N = 0.01$ in. measurements must be made over 1 in. downstream of the leading edge to have a pressure perturbation of less than 10 percent. Hence it is extremely important that the leading edge be made very sharp in order to eliminate the need for a blast effect correction.

If the disk probe is to be kept as small as possible, there obviously will be a requirement for the weak-interaction correction mentioned in previous sections and outlined step-by-step in Appendix II. Experimental confirmation of the weak-interaction correction for a disk probe is not available. Also, because of possible inflow/outflow effects, calibrations should be made. In addition, it is necessary to establish the magnitude of the plate misalignment in situ and to account for the effect of Mach number on the resulting pressure perturbation. A procedure to evaluate the plate misalignment is detailed in Appendix III, and the alignment factor deduced is incorporated in Appendix II.

Measurements made with a flat-plate probe (disk surface orthogonal to plane of streamline curvature) are subject to the complicating influence of multiple wave reflections. Previously, a calibration curve was determined to correct for the reflection of the model bow wave from the flat-plate probe surface. This curve was simply the overall pressure ratio across a single, reflected oblique shock related to the pressure rise across a single oblique shock. That this procedure, moreover, will also work for more than one wave is illustrated by the example shown in Fig. 15. It may be observed that there is a slight error (less than 2 percent) accumulated by zone 3 as a result of the more efficient compression (three shocks versus one). It should be noted, however, that this method of measurement is inherently less satisfactory than with the plate rolled 90 deg because the pressure rise will be twice its actual value. This only aggravates the shock wave boundary-layer interaction problem by roughly doubling the region of influence (Ref. 17). Consequently, there appears to be no valid reason for using a disk probe in any orientation other than parallel to the plane of streamline curvature.

This probe has the same problem as the cone in that uniform inviscid flow at the measurement station cannot be assumed to exist at subsonic and transonic speeds. Therefore calibrations must be made for this range of conditions.

SECTION III
CONCLUSIONS

The aerodynamic characteristics of conventional static-pressure measuring probes have been examined in detail to evaluate the influence of Mach number, angle of attack, Reynolds number, and orifice location. Based upon results presented, the following specific conclusions are of significance.

1. Cone-Cylinder Probe:

   (a) This probe is best for measurements ranging from subsonic and beyond and that by locating the measurement orifices at $\omega \approx \pm 40$ deg, circumferentially from the windward generator, the probe will be relatively insensitive to positive flow inclination at $0 < M < 4$. At hypersonic Mach numbers the circumferential location for minimal sensitivity, however, tends toward $\omega = 90$ deg.

   (b) The nose shape is not crucial, but it should be sharp, and the axial location of the measurement orifices should be at least 8 diameters aft of the nose junction with the cylinder.

   (c) Any enlargement in diameter downstream of the measurement orifices should be restricted to no more than 10-deg flare (semiangle) and should be at least 8 diameters downstream.

   (d) The error induced by positive flow inclination for $\omega \approx \pm 40$ deg tends to indicate local pressures higher than actually do exist when $M > 4$ (e.g., at $\alpha = 10$ and $M = 8$, about 115 percent).

(c) It is indicated that the effects of Reynolds number may be satisfactorily accounted for using a weak-interaction correction based on limited hypersonic data. This requires pitot probe data to be obtained simultaneously.

2. Sharp-Cone Probe:

   (a) Pitot probe measurements are required to infer the local static pressure from surface pressure measurements regardless of the significance of viscous effects.

   (b) The circumferential position of measurement for insensitivity to positive flow inclinations increases about 20 deg in the Mach number range from 2 to 8. A good compromise location is with a pair of orifices situated ±85 deg circumferentially from the windward ray.

   (c) The effects of self-induced pressure perturbations must be considered, and the inviscid, cone pressure may be estimated using a cone, weak-interaction correction.

   (d) The error induced by positive flow inclination of 10 deg for $\omega = \pm 85$ deg will indicate pressures which are lower than the true static pressure by about 15 percent at M = 2 but which are approximately correct at M = 8. The characteristics of cones at $M \lesssim 2$ are uncertain.

3. Planar Probe:

   (a) Because of the significance of viscous effects on the measured pressure, pitot pressure measurements are required simultaneously in order to implement flat-plate weak-interaction corrections. Experimental confirmation of the weak-interaction correction and examination of posssible inflow/outflow effects are needed for disk probes.

   (b) The probe should be used with its surface parallel to the plane of flow inclination ($\phi = 90$ deg) in order to minimize shock wave boundary-layer interaction effects and the need for a calibration curve.

   (c) The primary shortcoming of this probe is its sensitivity to angle of yaw misalignment. To compensate for this perturbation, independent measurements (either surface or free stream) are required in order to account for the effect of Mach number.

   (d) Care must be exercised at hypersonic speeds to ensure that the leading edge is sufficiently sharp so that blast-wave-induced pressures are insignificant at the orifice location.

(e) The error induced by a positive yaw setting error of 0.5 deg (considered an achievable alignment precision) will be no more than about 10 percent at M = 8 and 2 percent at M = 2.

As a result of the above considerations, it is concluded that the planar probe and the sharp-cone probe are equally capable of yielding more accurate local static-pressure measurements than the cone-cylinder probe at supersonic and hypersonic speeds ($4 \leqslant M \leqslant 8$). However, in the range of $0 < M < 4$, the cone-cylinder probe will yield the most accurate results, in general, and allow measurements to be made at the lowest Mach number.

REFERENCES

1. Bryer, D. W., Walshe, D. E. and Garner, H. C. "Pressure Probes Selected for Three-Dimensional Flow Measurement." ARC R & M 3037, 1958.

2. Prandtl, L. and Tietjens, O. G. Applied Hydro- and Aeromechanics. Dover Publications, Inc., New York, New York, 1957.

3. Liepmann, H. W., Roshko, A. and Dhawan, S. "On Reflection of Shock Waves from Boundary Layers." NACA Report 1100, 1952.

4. Pope, Alan and Goin, Kenneth L. High-Speed Wind Tunnel Testing. John Wiley & Sons, Inc., New York, New York. 1965.

5. Martellucci, A., Ranlet, J., Schlesinger, A., and Garberoglio, J. "Experimental Study of Near Wakes– Part I–Data Presentation." General Applied Sciences Laboratories (GASL) - TR-641, March 1967.

6. Washington, William D. and Humphrey, James A. "Pressure Measurements on Four Cone-Cylinder-Flare Configurations at Supersonic Speeds." RD-TM-69-11 (AD 699359), October 1969.

7. Eaves, R. H., Jr. "An Empirical Correlation of Pressure on Blunt-Nosed Cylindrical Afterbodies at Hypersonic Mach Numbers." AEDC-TR-68-82 (AD669565), May 1968.

8. Williams, M. J. "Static Pressure Probes at Mach Number 7.5." Aero Note 327, Australian Defense Scientific Service, September 1970.

9. Walter, L. W. and Redman, E. J. "Needle Static Pressure Probes Insensitive to Flow Inclination in Supersonic Air Streams." Naval Ordnance Lab Report 3694 (AD37422), March 1954.

10. Jones, Robert T. "Effects of Sweepback on Boundary Layer and Separation." NACA Report No. 884, 1947.

11. Gowen, Forrest E. and Perkins, Edward W. "Drag of Circular Cylinders for a Wide Range of Reynolds Numbers and Mach Numbers." NACA TN 2960, June 1953.

12. Penland, Jim A. "Aerodynamic Characteristics of a Circular Cylinder at Mach Number 6.86 and Angles of Attack up to 90°." NACA TN 3861, January 1957.

13. Matthews, Malcolm L. "An Experimental Investigation of Viscous Effects on Static and Impact Pressure Probes in Hypersonic Flow." Guggenheim Aeronautical Laboratory (GALCIT) Memorandum No. 44, June 2, 1958.

14. Behrens, W. "Viscous Interaction Effects on a Static Pressure Probe at M = 6." AIAA Journal, Vol. I, No. 12, December 1963, pp. 2864-2866.

15. Cox, R. N. and Crabtree, L. F. Elements of Hypersonic Aerodynamics. Academic Press, New York, 1965.

16. Boylan, David E. "An Analysis of Initial Static Pressure Probe Measurements in a Low-Density Hypervelocity Wind Tunnel." AEDC-TDR-63-94 (AD402935), April 1963.

17. Gray, J. Don. "Investigation of the Effect of Flare and Ramp Angle on the Upstream Influence of Laminar and Transitional Reattaching Flows from Mach 3 to 7." AEDC-TR-66-190 (AD645840), January 1967.

18. Jones, D. J. "Tables of Inviscid Supersonic Flow about Circular Cones at Incidence γ = 1.4." AGARDograph 137, November 1969.

19. Norris, John D. "Calibration of Conical Pressure Probes for Determination of Local Flow Conditions at Mach Numbers from 3 to 6." NASA TN D-3076, November 1965.

20. Talbot, L., Koga, T. and Sherman, P. M. "Hypersonic Viscous Flow over Slender Cones." NACA TN-4327, September 1958.

21. Liepman and Roshko. Elements of Gasdynamics. John Wiley & Sons, Inc., 1957.

APPENDIXES

I. ILLUSTRATIONS
II. WEAK-INTERACTION AND ALIGNMENT CORRECTION PROCEDURE
III. PROCEDURE FOR EVALUATING THE PLATE ALIGNMENT FACTOR

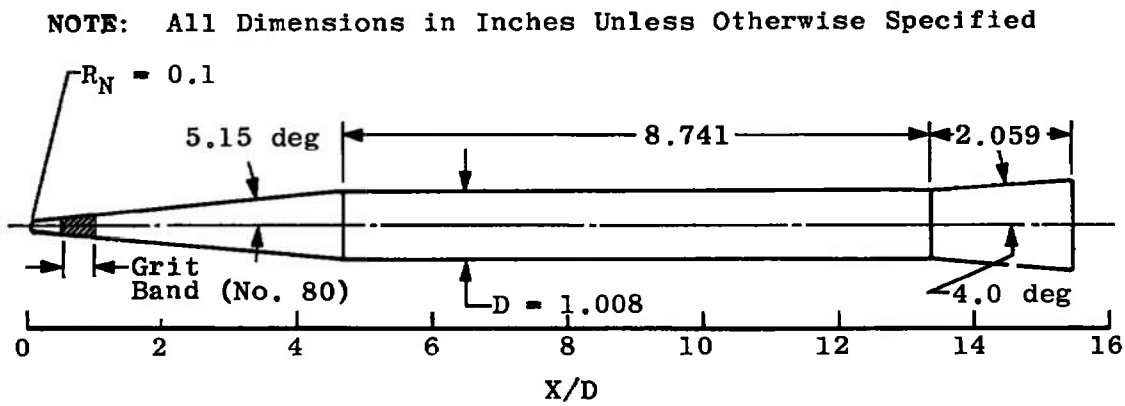

Model Configuration (No. 2 of Ref. 6)

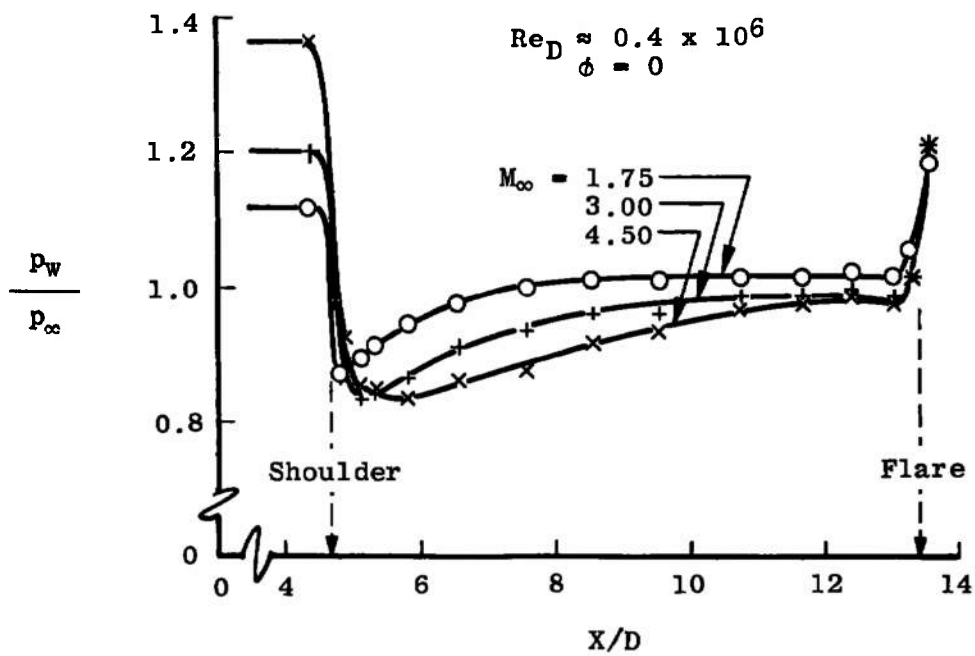

Fig. 1 Typical Effect of Mach Number on the Longitudinal Surface Pressure Distribution on a Slender Cone-Cylinder Model at α = 0

Data Source: Ref. 6. Model No. 2

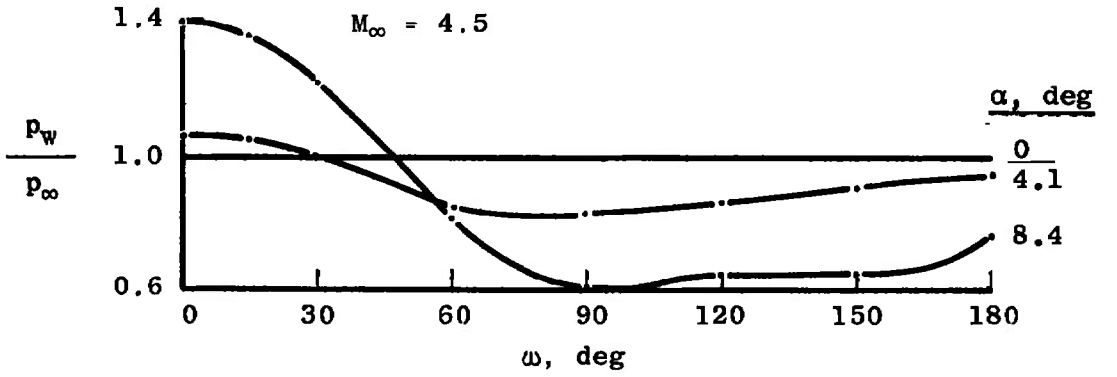

a. Angle-of-Attack Variation

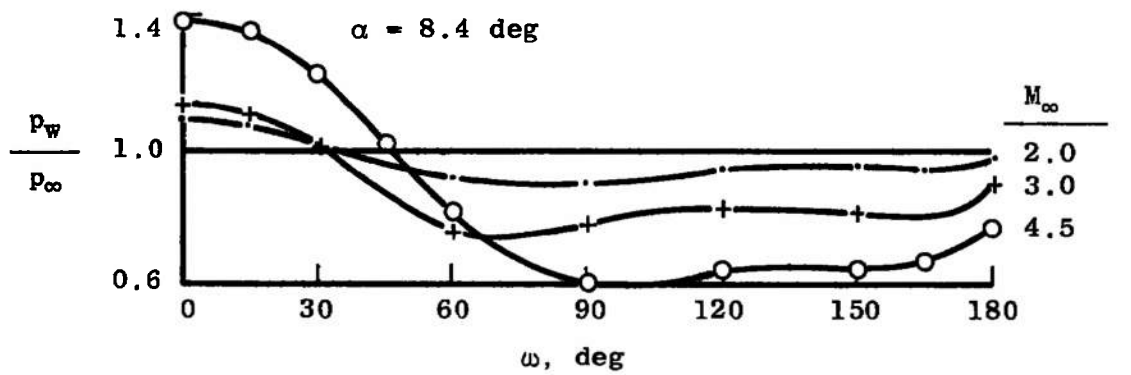

b. Mach Number Variation

Fig. 2 Effects of Mach Number and Angle of Attack on the Circumferential Pressure Variation of a Slender Cone-Cylinder at X/D = 13

Data Source: Ref. 6, Model No. 2

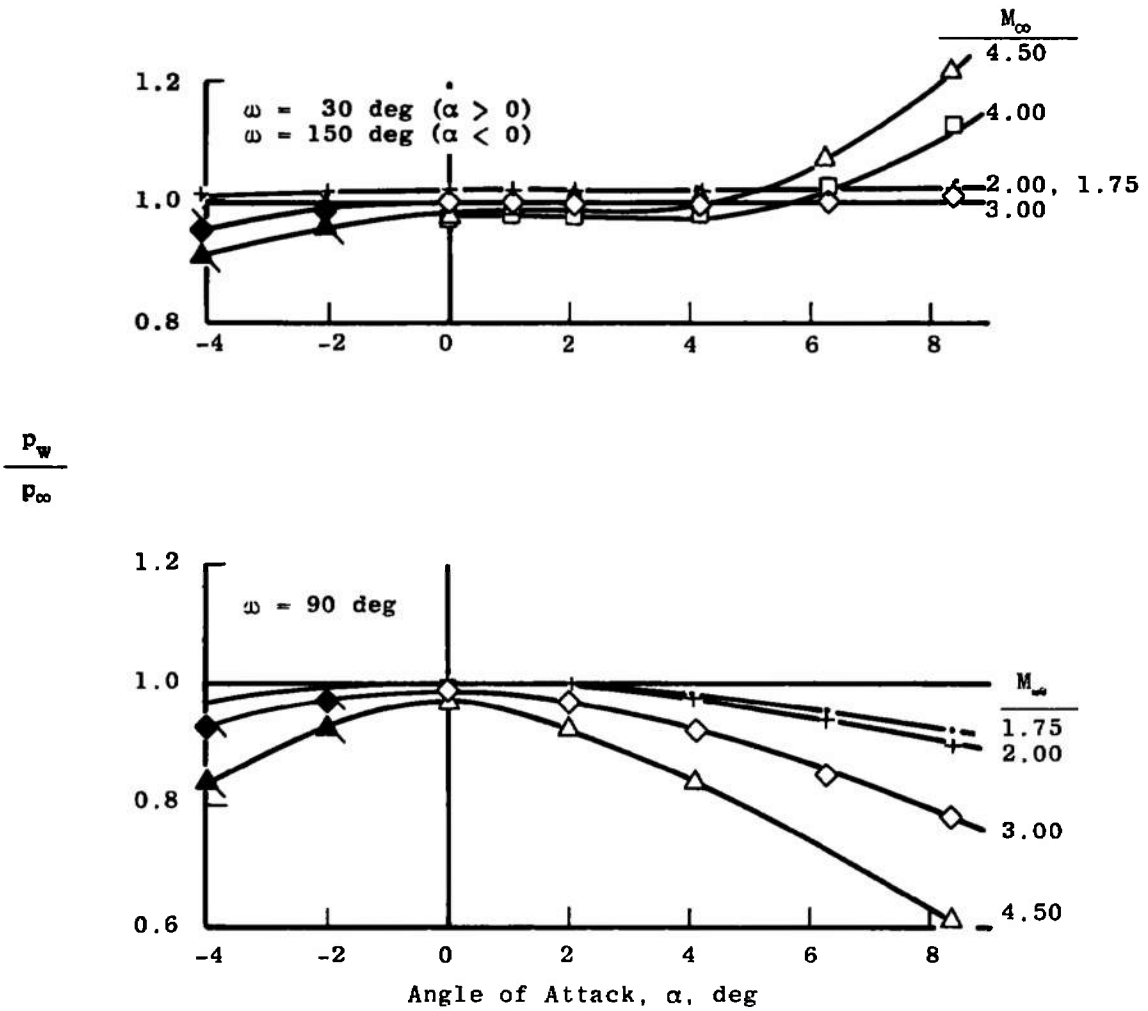

Fig. 3 Effects of Mach Number and Circumferential Location on the Pressure Ratio Variation with Angle of Attack for a Cone-Cylinder at X/D = 13

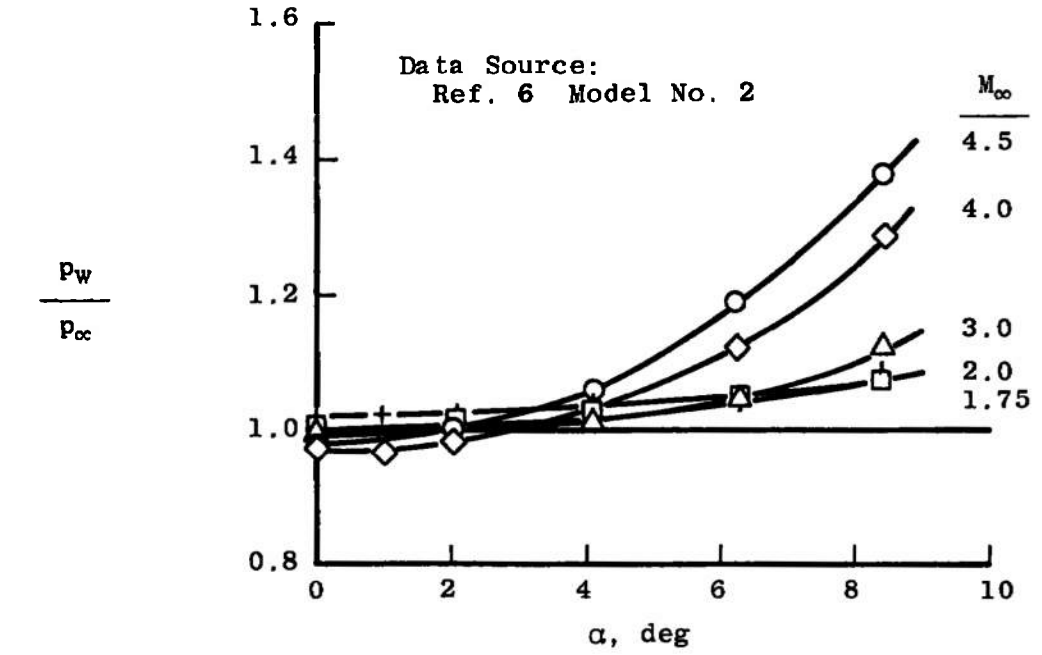

a. Basic Data, X/D = 13

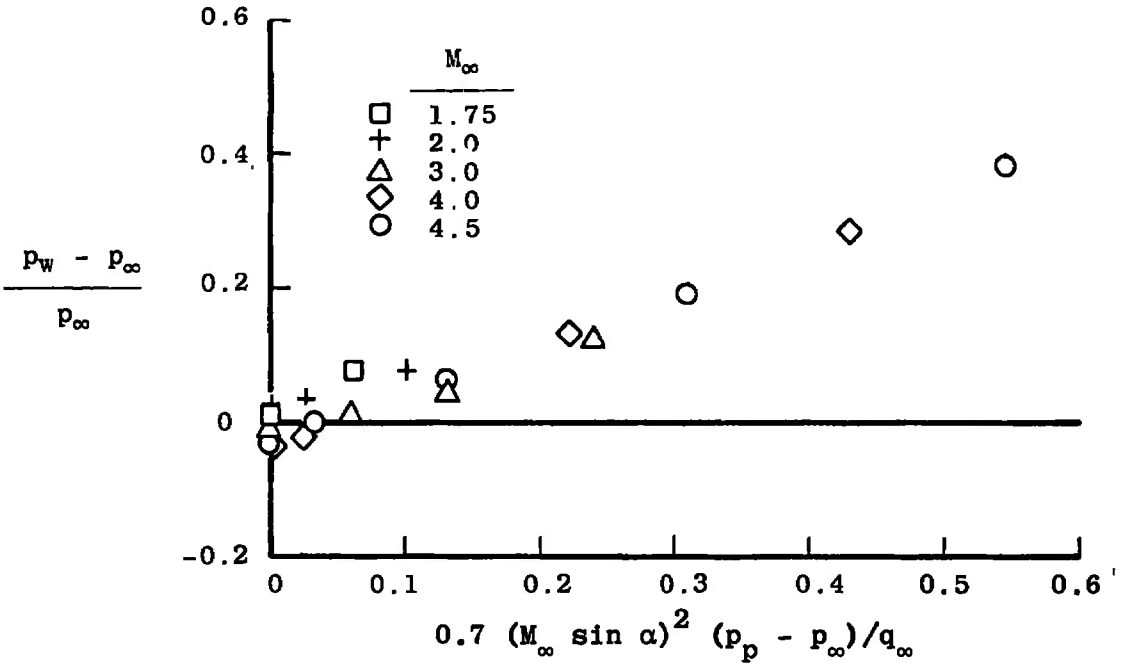

b. Newtonian Correlation of Basic Data

Fig. 4 Influence of Mach Number on the Maximum Sensitivity of Cylinder Pressure Ratio to Angle-of-Attack Variation, $\omega = 0$

Data Sources: Refs. 11 and 12

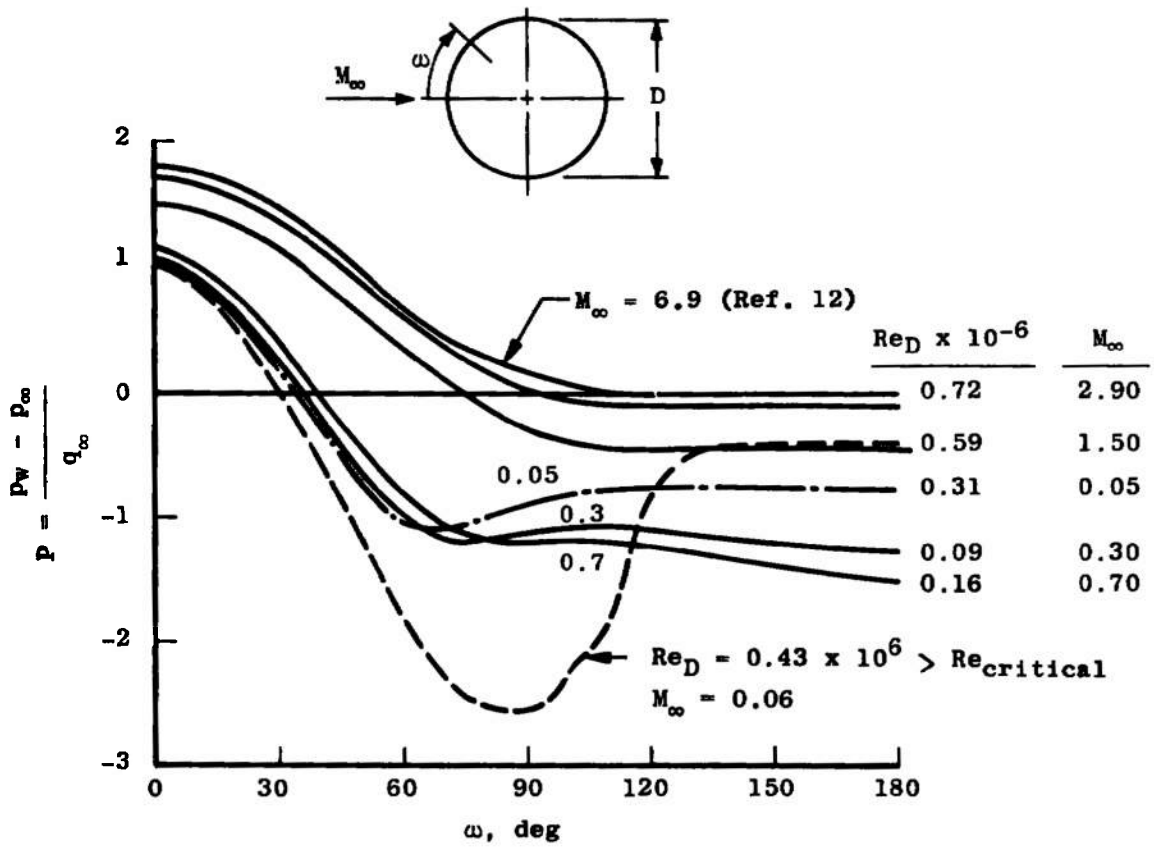

Fig. 5 Circumferential Pressure Distributions for Cylinders Normal to Flow, Experimental Results

Transformation Expression:

$$\frac{p_w}{p} = 1 + \frac{\gamma}{2} M^2_{normal} P$$

where $P = P(M_{normal}, \omega)$, see Fig. 5

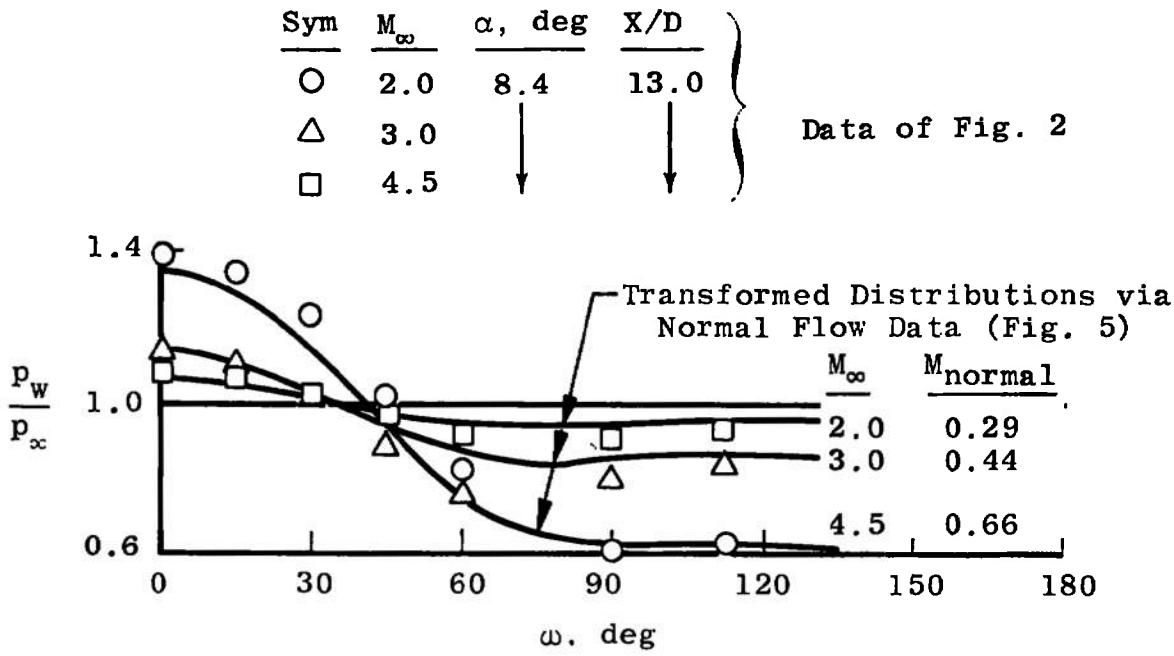

Fig. 6 Comparison of Yawed Cone-Cylinder Circumferential Pressures with Transformed Distributions of Cylinders in Normal Flow

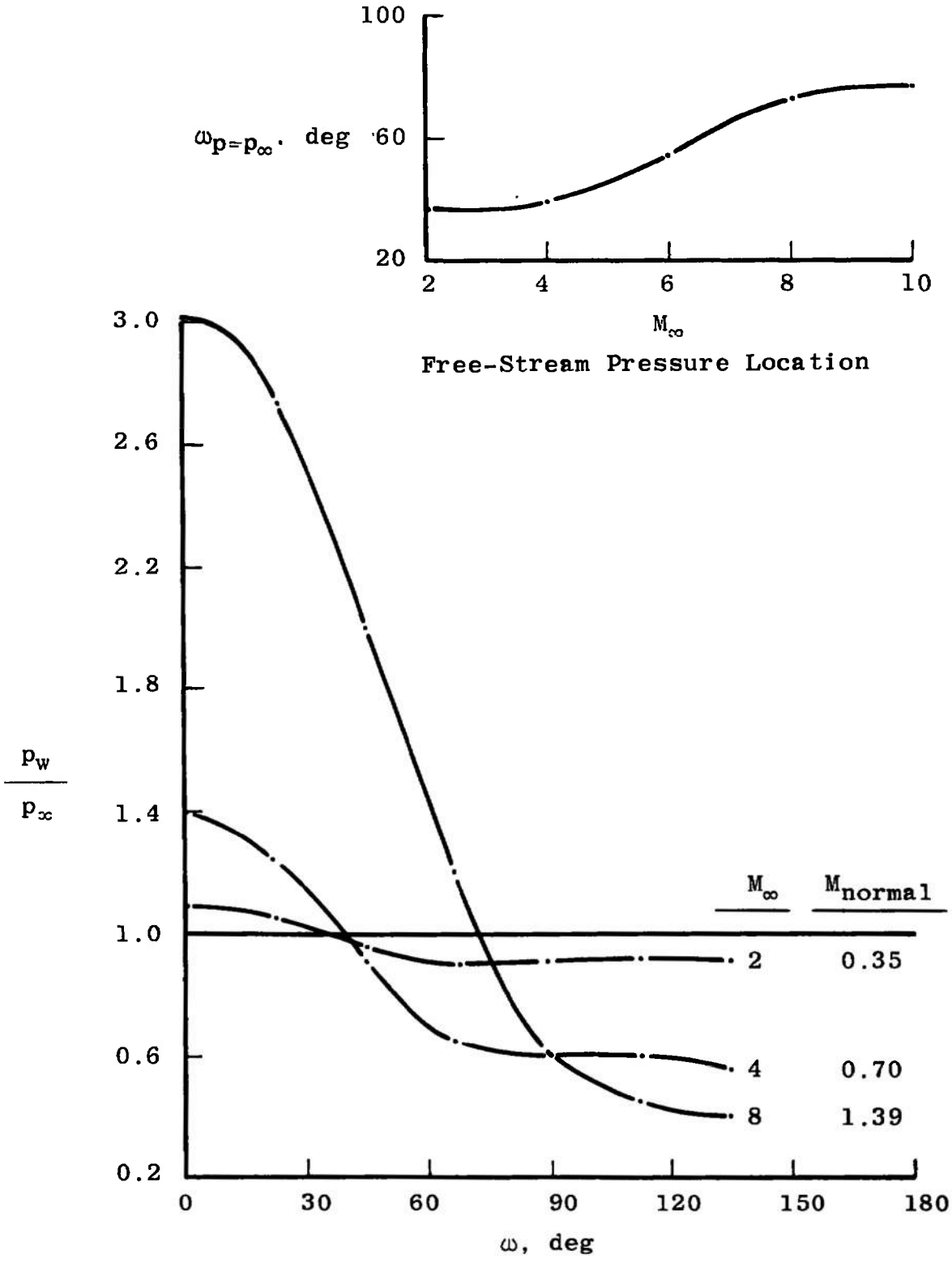

Fig. 7 Effects of Mach Number on Circumferential Cylinder Pressures at α = 10 deg Predicted by the Transformation of Normal Flow Data

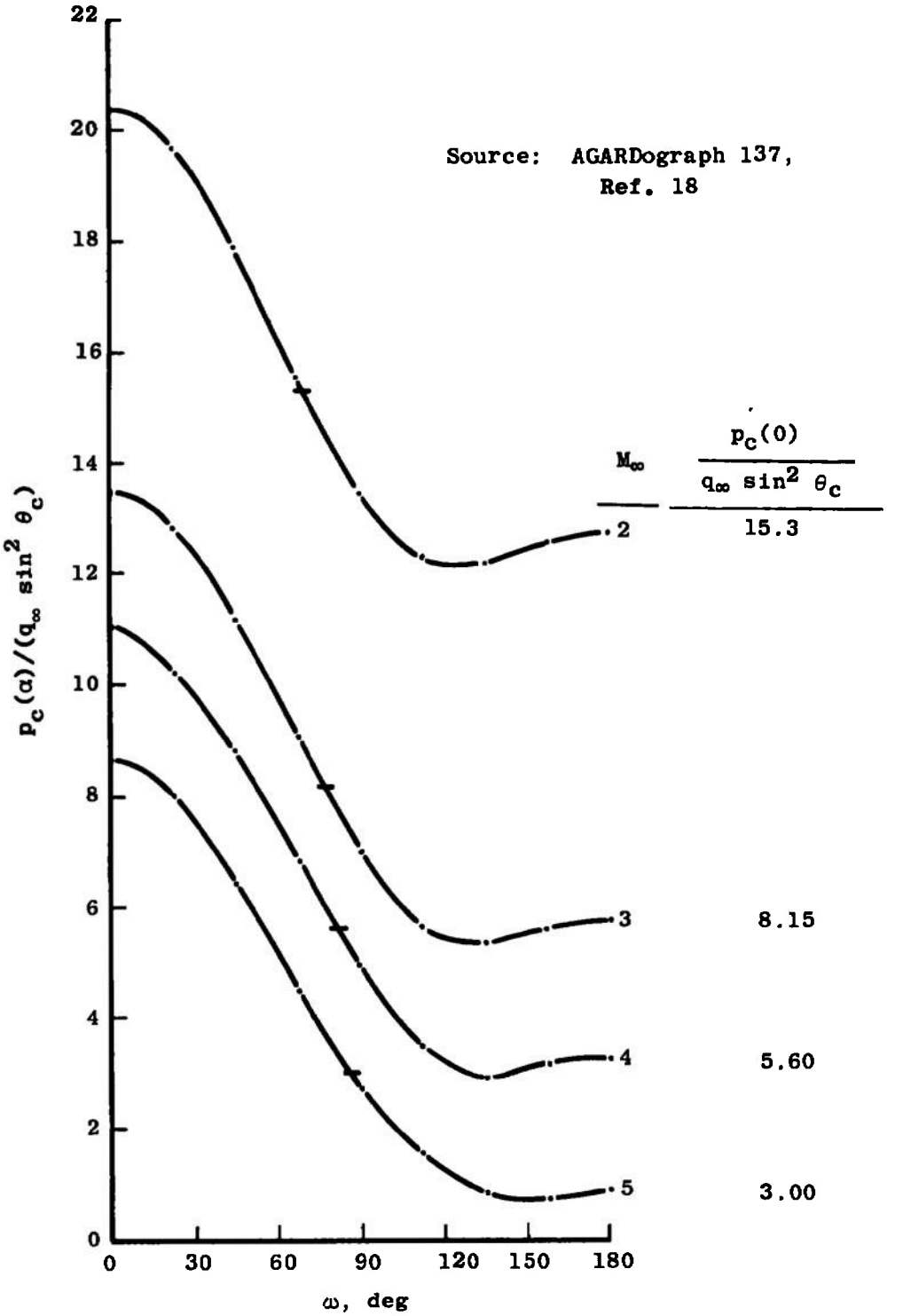

a. Absolute Variation, Inviscid

Fig. 8 Effects of Mach Number on the Circumferential Pressure Variation of a 10-deg (Semiangle) Cone at α = 10 deg

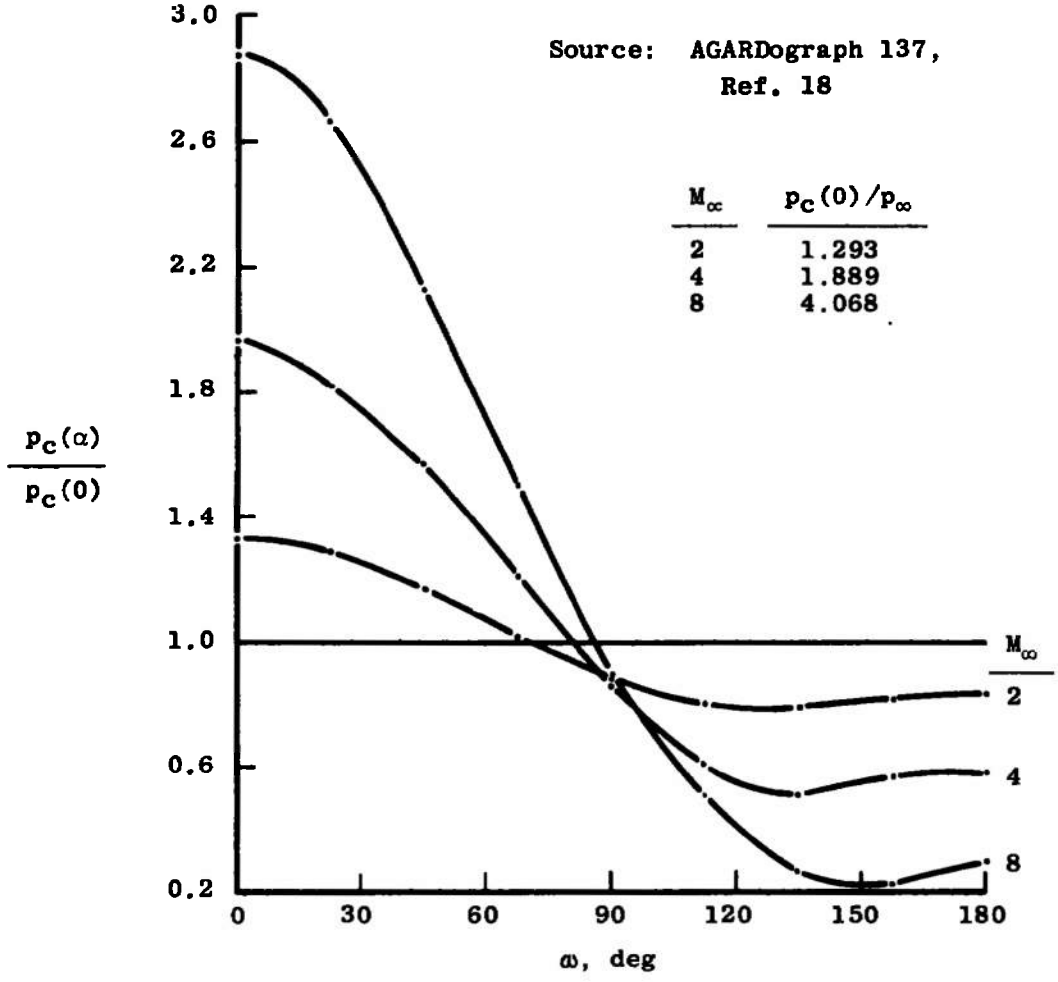

b. Variation Relation to Unyawed Level, Inviscid
Fig. 8 Concluded

Source: AGARDograph 137, Ref. 18

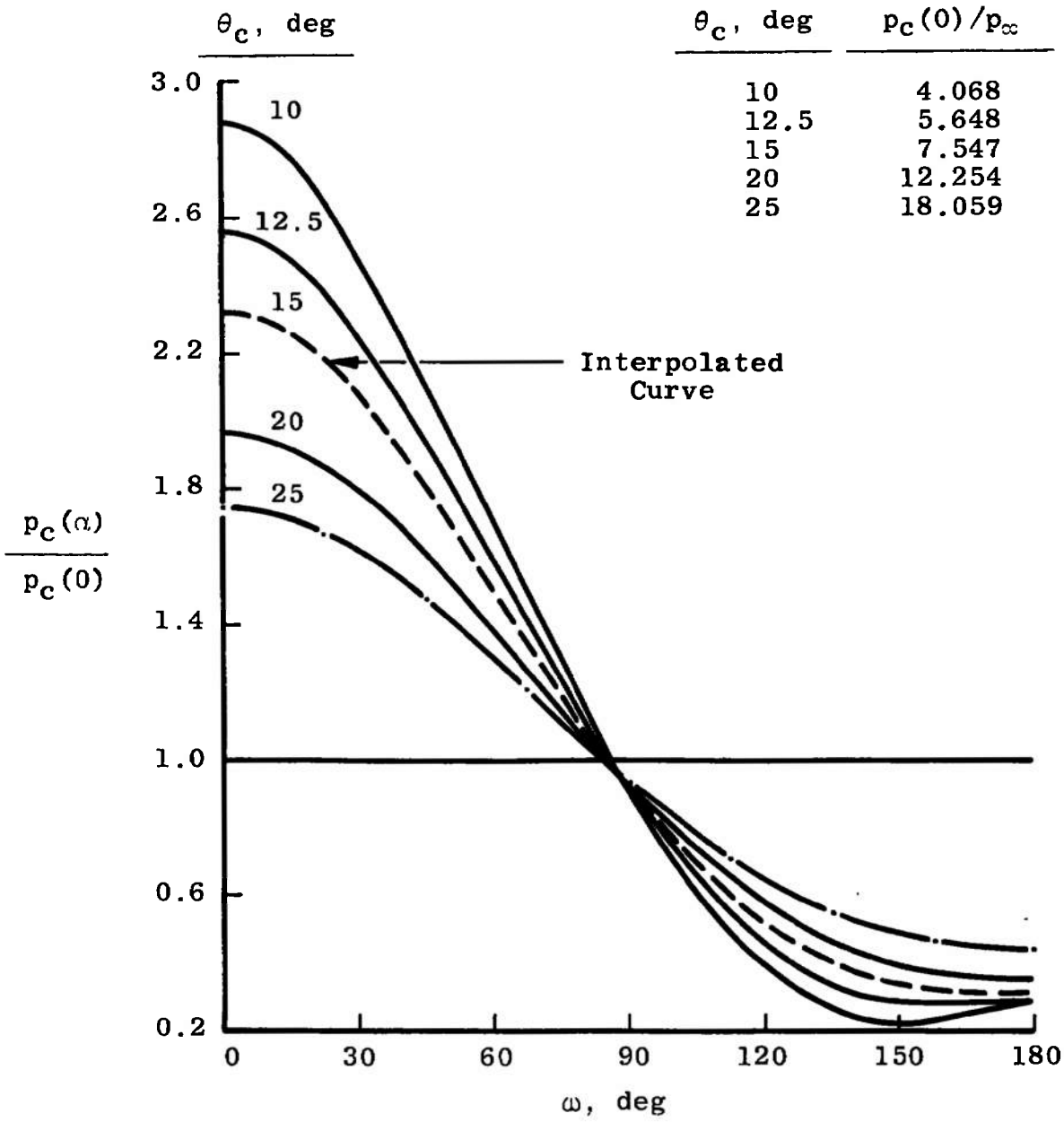

Fig. 9 Effect of Cone Semiangle on the Circumferential Pressure Variation at $M_\infty = 8$ and $\alpha = 10$ deg

Source: AGARDograph 137, Ref. 18

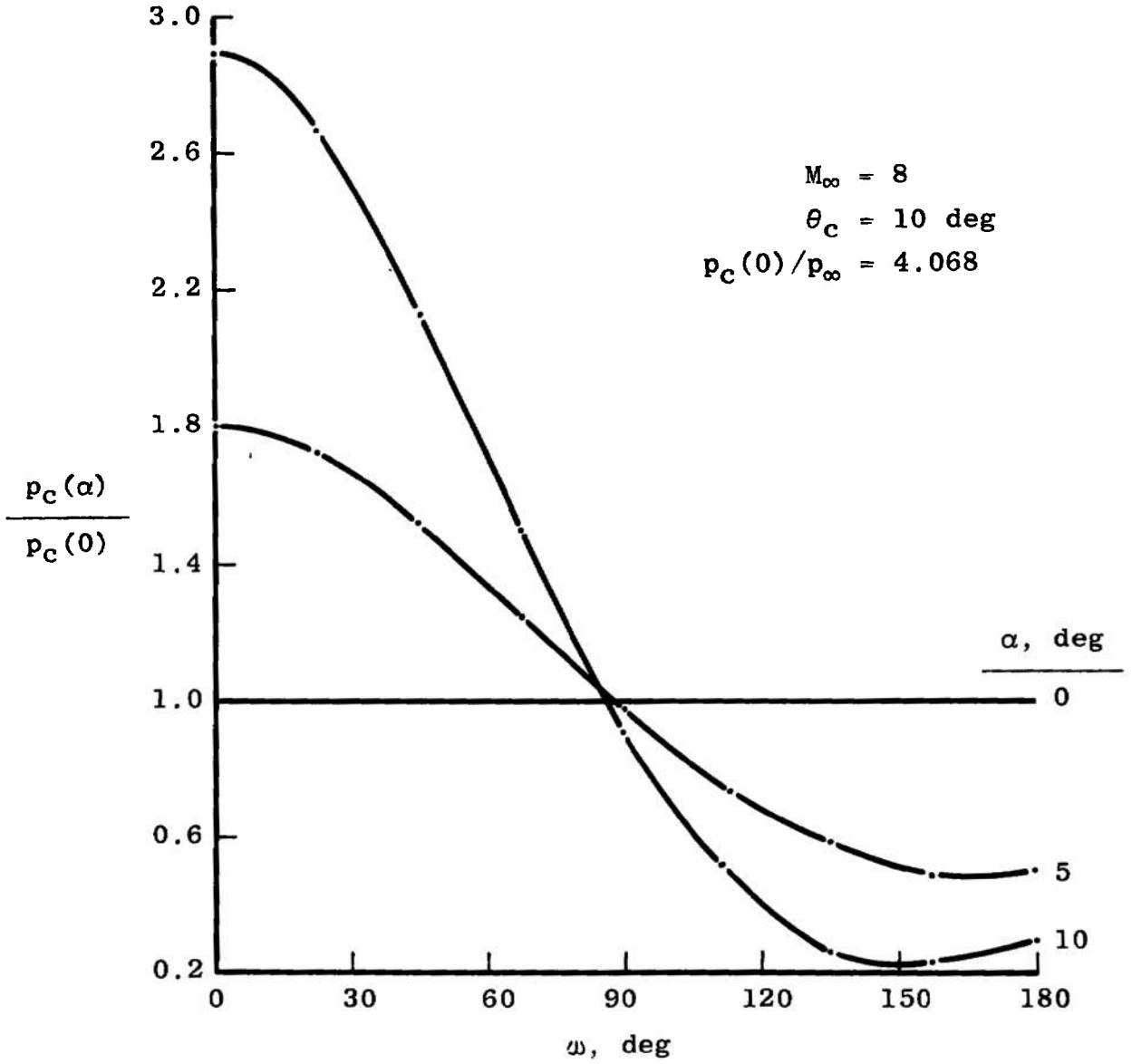

a. Circumferential Variation

Fig. 10 Effect of Angle of Attack on Cone Pressures

Source: AGARDograph 137, Ref. 18

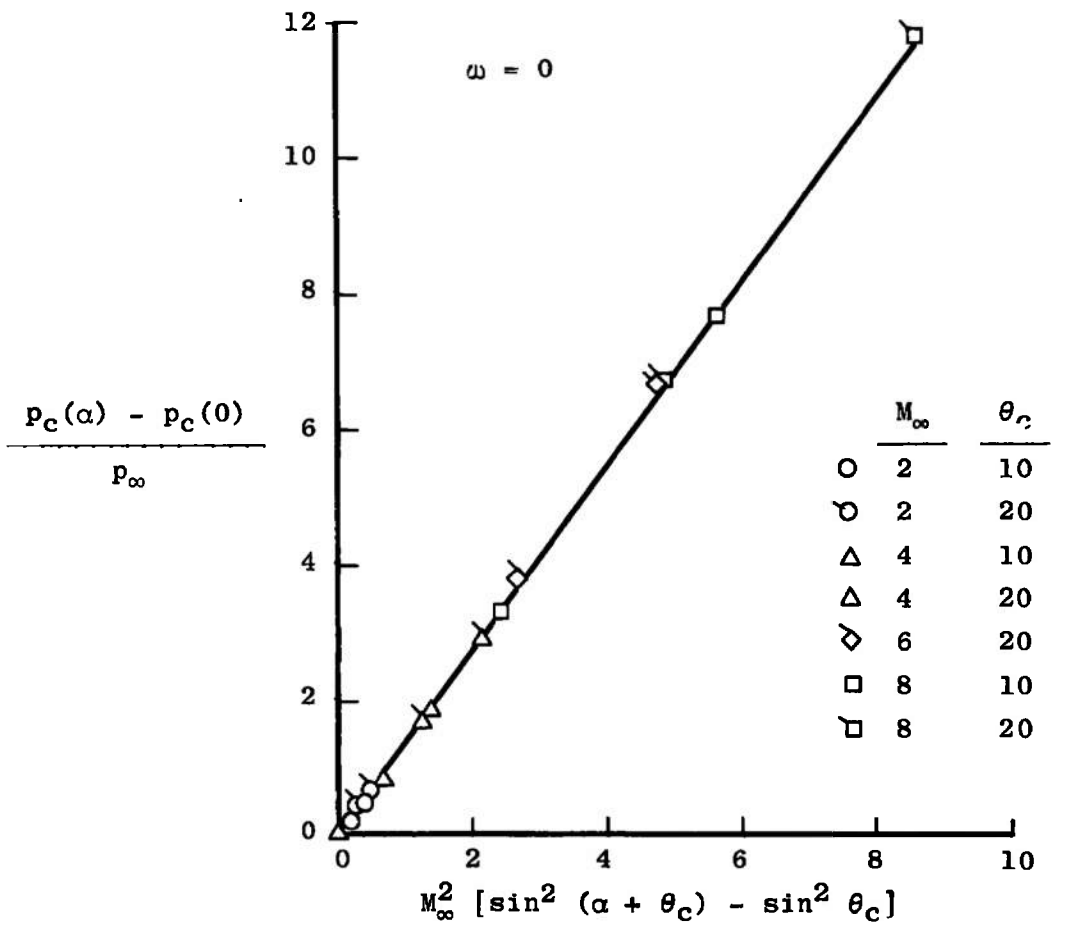

b. Hypersonic Correlation of the Maximum Increment
Fig. 10 Concluded

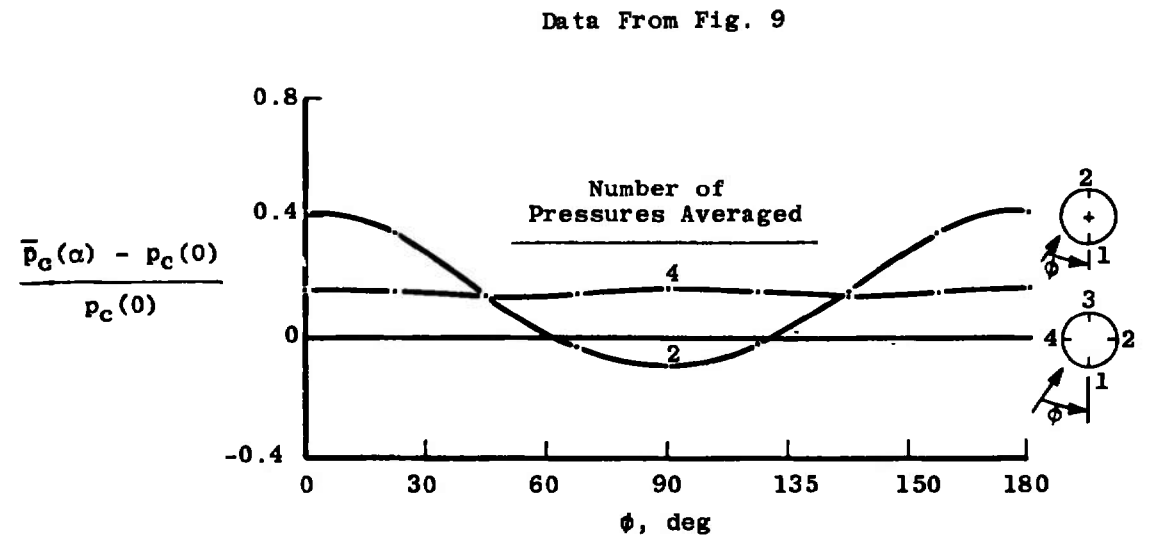

a. Relative to Unyawed Cone

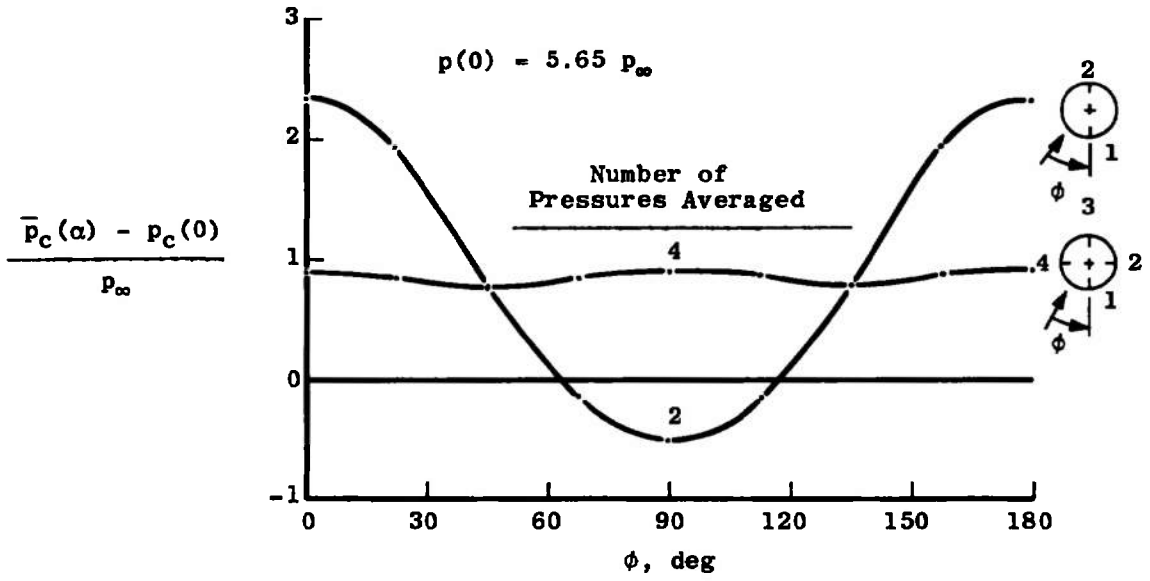

b. Relative to Free Stream

Fig. 11 Influence of Roll Orientation on Averages of Cone Pressure at 10-deg Yaw (M_∞ = 8 and θ_c = 12.5 deg)

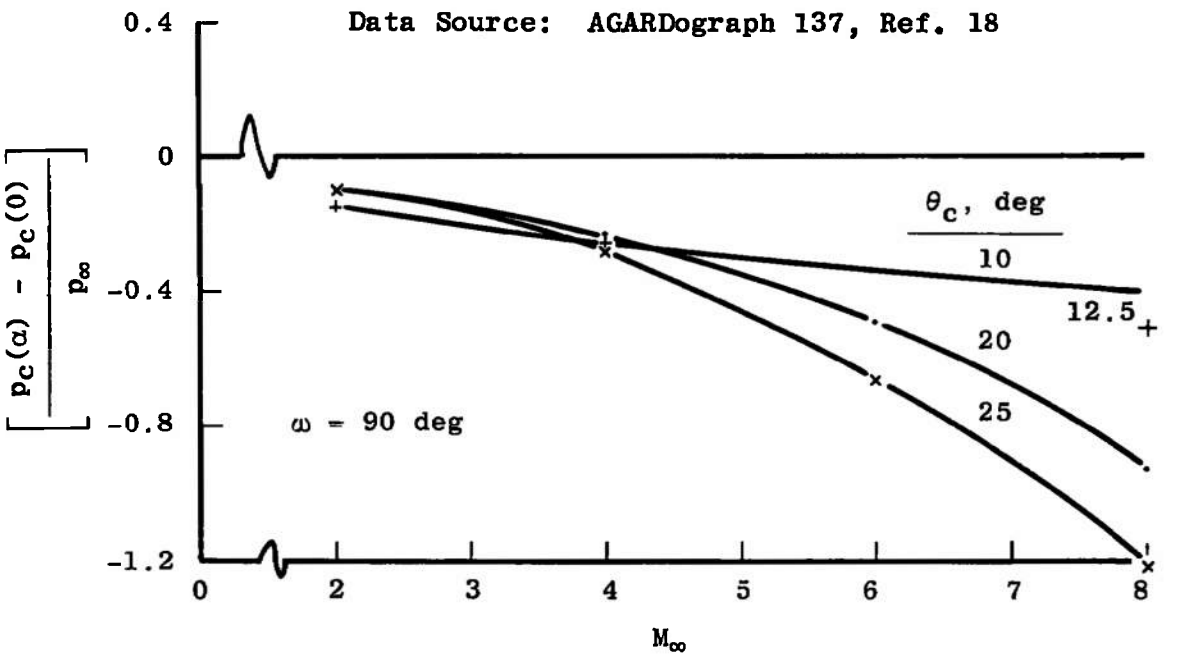

Fig. 12 Effects of Mach Number and Cone Angle on the Pressure Increment Measured at α = 10 deg

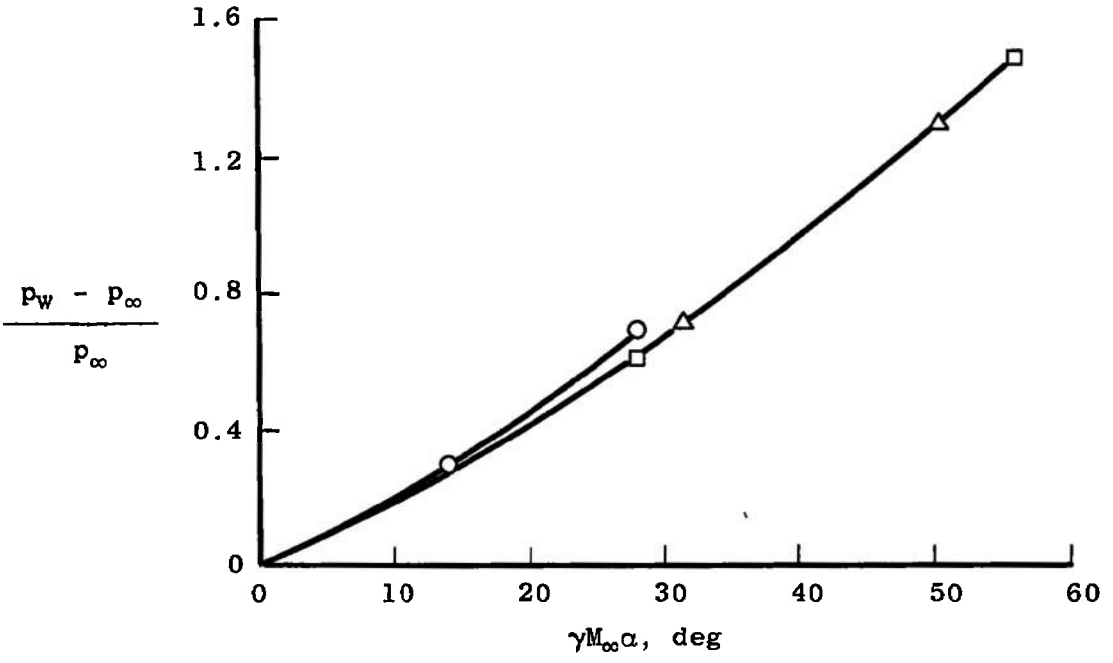

a. Hypersonic Approximation

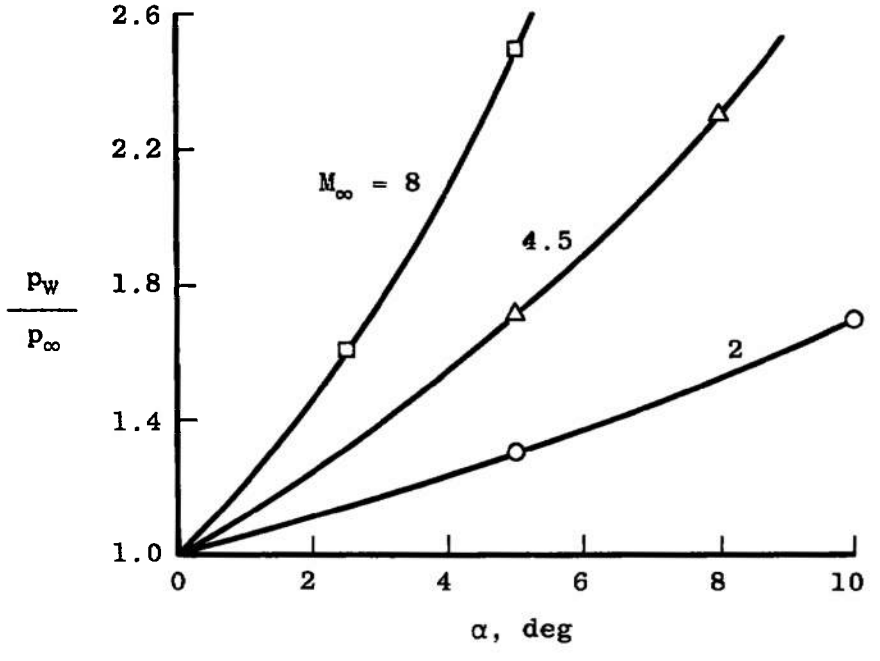

b. Isentropic Pressure Ratio

Fig. 13 Influence of Mach Number on the Maximum Sensitivity of Flat-Plate Pressure to an Angle of Attack, Inviscid Flow

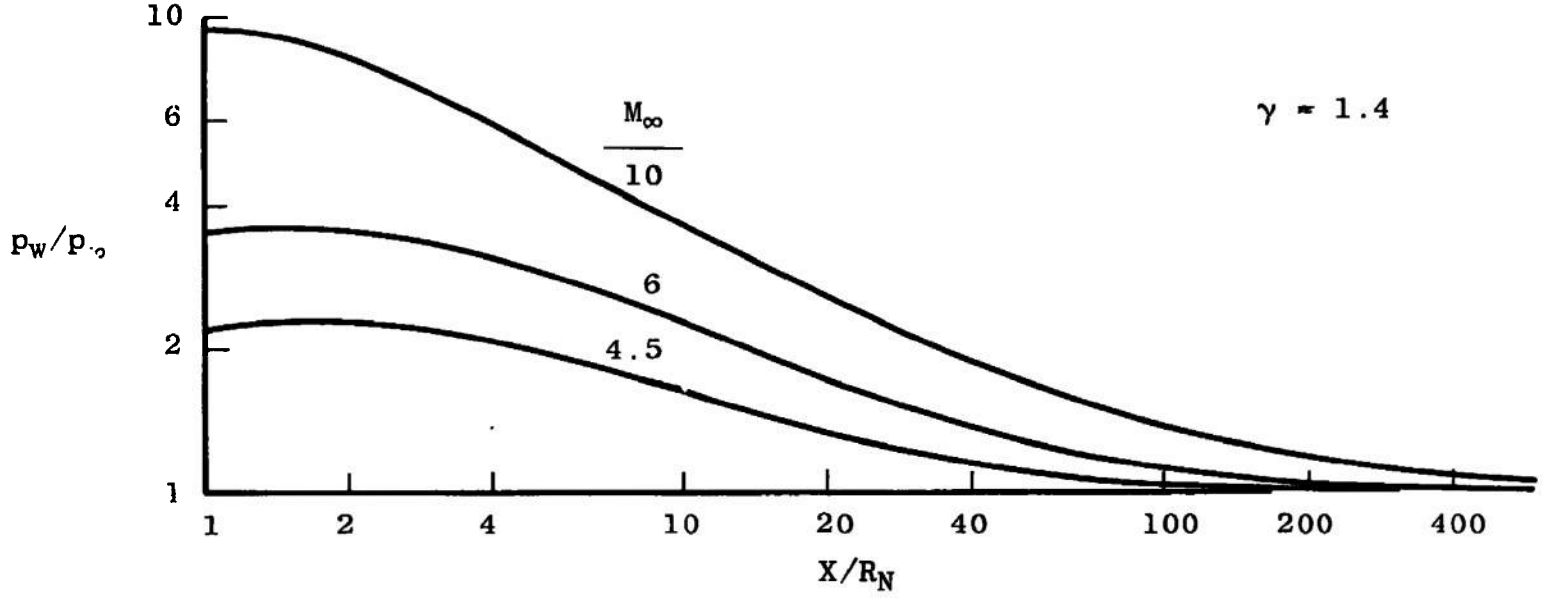

Fig. 14 Effects of Mach Number on the Influence of Nose Bluntness on Inviscid Pressures on a Flat Plate, $\alpha = 0$

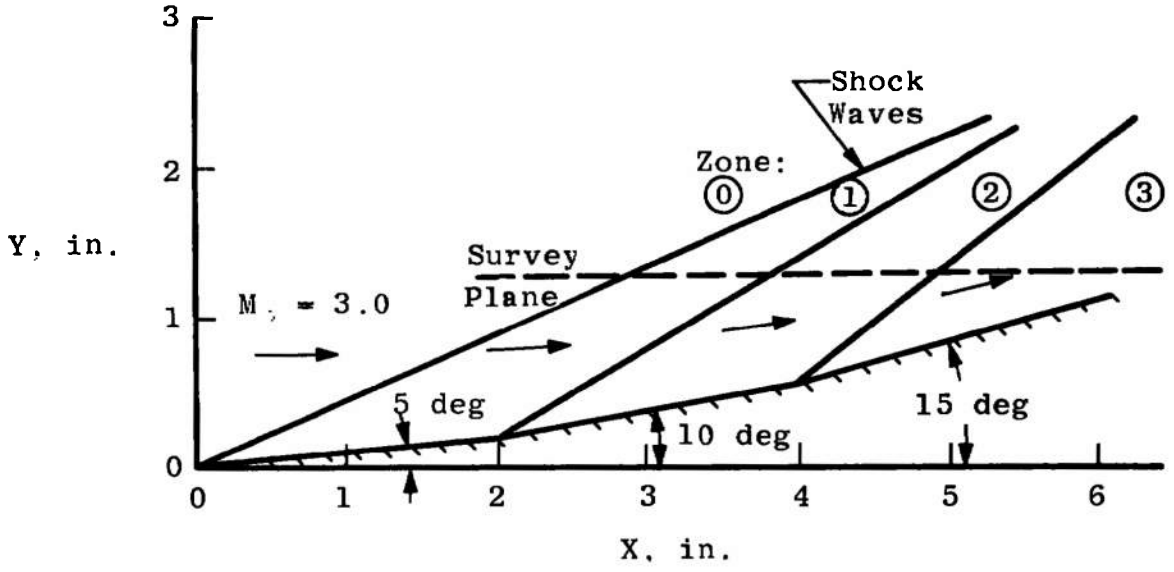

a. Multiple Shock Flow Field

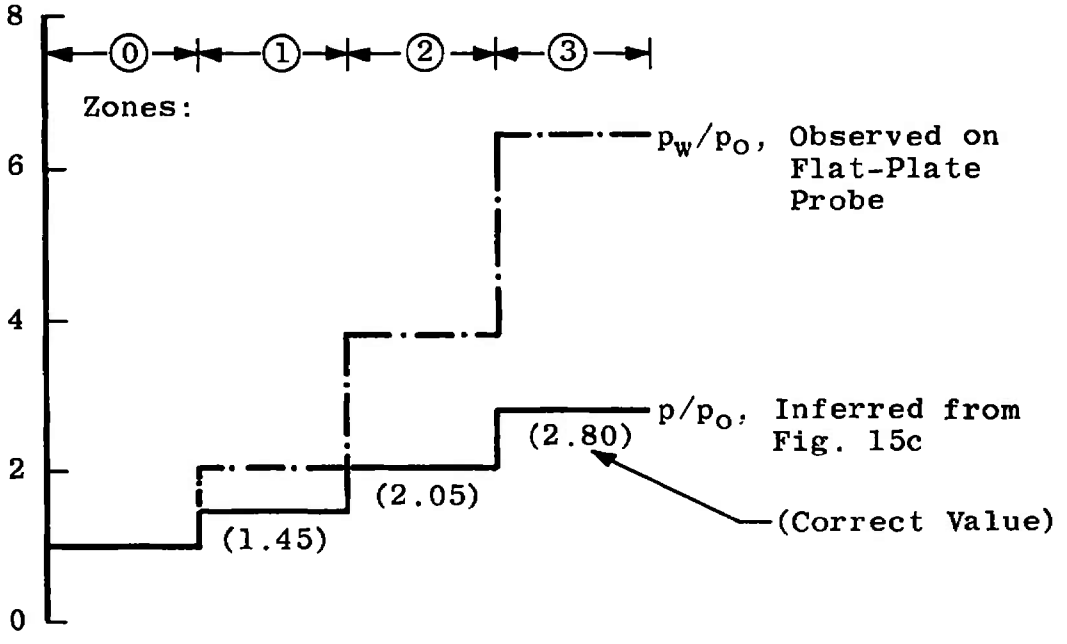

b. Comparison of Results

Fig. 15 Example of the Applicability of Flat-Plate Measurements in Multiple Shock Flows Using Single Shock Calibration Curve, a Theoretical Analysis

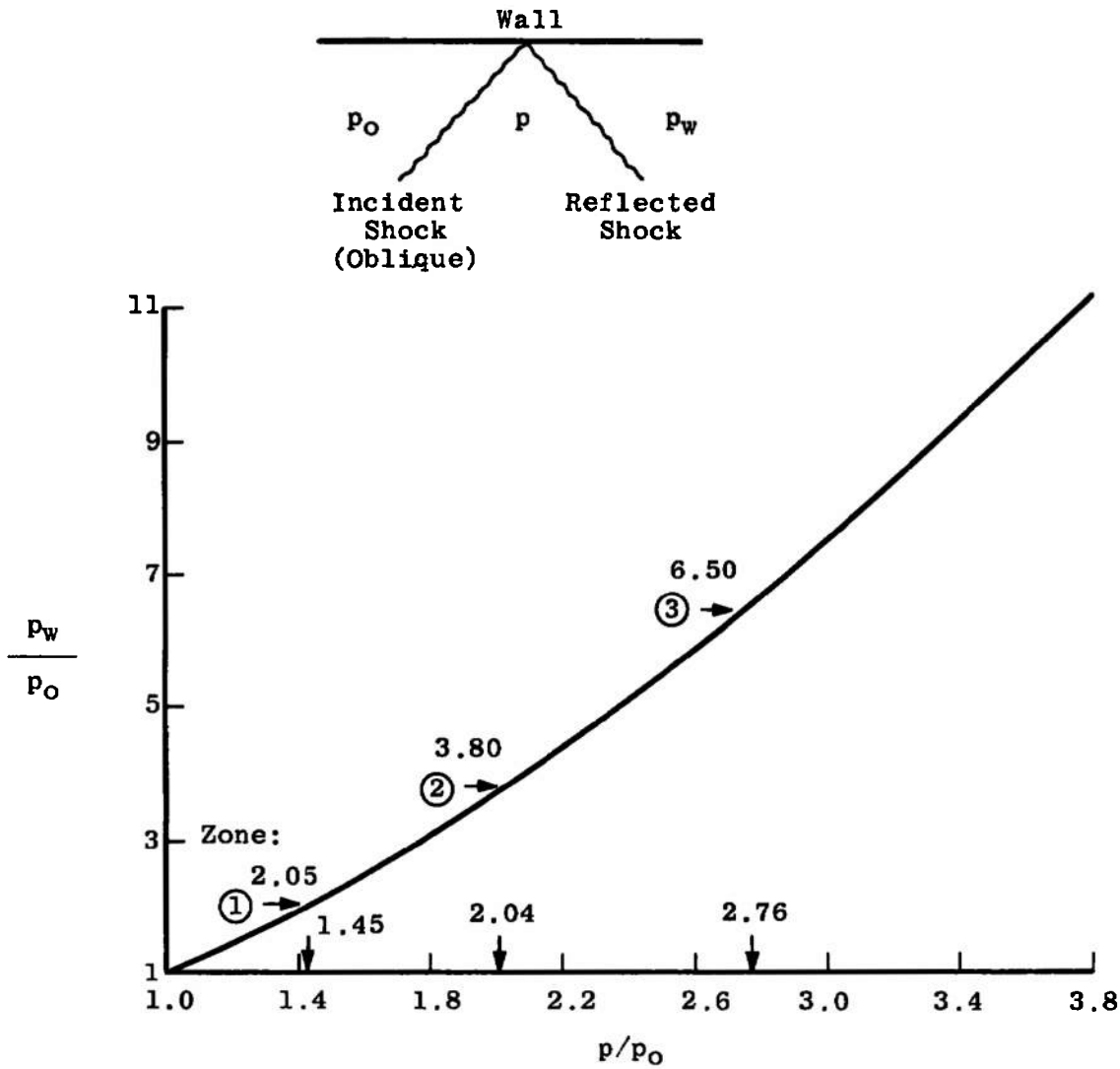

c. Single Shock Calibration Curve
Fig. 15 Concluded

APPENDIX II
WEAK-INTERACTION AND ALIGNMENT CORRECTION PROCEDURE

Data are assumed available for the same coordinates in space in the form of

p_p = pitot probe pressure, psia

p_w = static probe pressure, psia

It is required that the wetted distance from the tip of the probe to the wall orifice, ℓ, be specified, and also in the case of conical probes that the inviscid flow conditions on the surface appropriate to the cone angle be available in the form of a power series in Mach number, for example. It is considered necessary to correct plate (disk) readings for both viscous and angle-of-attack effects, because of the great difficulty in verifying the in situ alignment of this type of probe. A special procedure is required to deduce the amount of the plate misalignment which is incorporated in this correction procedure. The evaluation of it is described in Appendix III.

The correct local pressure is inferred through an iterative calculation which is begun by assuming that the local pressure is equal to the probe pressure; that is, let $p = p_w$ for the first iteration.

1. Determine the local Rayleigh or isentropic Mach number.

   a. When $p < 0.528\ p_p$, iterate for M using

$$p/p_p = \left(\frac{7M^2 - 1}{6}\right)^{2.5} \left(\frac{5}{6M^2}\right)^{3.5}$$

   b. When $p \geq 0.528\ p_p$, solve for M

$$M = \sqrt{5\left[\left(p_p/p\right)^{0.286} - 1\right]}$$

2. If a plate (disk) probe is used, account for the angle-of-attack effects using the value of K_α derived from calculations based on procedure in Appendix III. Note that p_{iw} is the inviscid wall pressure.

   a. When $M \geq 1.5$, use

$$p_{iw}/p = 1 + K_\alpha M^2/\sqrt{M^2 - 1}$$

   b. When $M < 1.5$, use

$$p_{iw}/p = 1 + 2K_\alpha M$$

3. Calculate the inviscid wall Mach number.

   a. For a plate probe, use

$$M_{iw} = \frac{\sqrt{M^2 + 5\left[1-(p_{iw}/p)^{0.286}\right]}}{(p_{iw}/p)^{0.143}}$$

   b. For a cylindrical probe ($\theta = 0$) or a conical probe of semiangle θ_c calculate the inviscid wall Mach number using a polynomial fit of theoretical data.

$$M_{iw} = a_o(\theta) + \sum_{n=1}^{m} a_n(\theta)M^n$$

4. If a cylindrical or conical probe is used, calculate the inviscid wall pressure ratio using a polynomial fit of inviscid theoretical data.

$$p_{iw}/p = b_o(\theta) + \sum_{n=1}^{m} b_n(\theta)M^n$$

   Ideally for a cylindrical probe, $b_o(0) = 1$ and $b_n(0) = 0$ for $n \geq 1$.

5. Calculate the inviscid wall Reynolds number parameter assuming a laminar, adiabatic wall temperature, T_w.

$$(Re_\ell/C)_{iw} = \frac{0.343\ell(p_{iw}/p)p\ M_{iw}(T_w/T_{iw})}{\mu_w T_{iw}^{0.5}}$$

   where:

$$T_{iw} = T_t \div \left(1 + 0.20\,M_{iw}^2\right)$$
$$T_w = T_{iw}\left(1 + 0.173\,M_{iw}^2\right)$$

   and if

   a. $T_w \leq 216°R$

$$\mu_w = 8.06\,T_w \times 10^{-10}$$

   b. $T_w > 216°R$

$$\mu_w = \frac{227\,T_w^{1.5} \times 10^{-10}}{T_w + 198.6}$$

6. Compute the viscous interaction parameter for the inviscid wall conditions.

$$\bar{\chi}_{iw} M_{iw}^3 \div \sqrt{(Re_{\ell}/C)_{iw}}$$

7. Calculate the ratio of the viscous to the inviscid wall pressure.

$$p_w/p_{iw} = 1 + A\bar{\chi}_{iw}$$

where

a. For plates and cylinders, use A = 0.45 (Ref. 21, p. 344)

b. For cones, use A = 0.14 (Ref. 20)

8. Compute the ratio of the probe to local pressure.

$$\frac{p_w}{p} = \frac{p_w}{p_{iw}} \frac{p_{iw}}{p}$$

9. Calculate the inferred local pressure.

$$p = p_w \div (p_w/p)$$

10. Evaluate the absolute change of the inferred pressure from iteration (n - 1) to iteration (n) and check for convergence to a satisfactory tolerance, say ϵ the estimated transducer uncertainty. If $|p(n) - p(n-1)| < \epsilon$ stop iteration. If equal to or greater than ϵ, repeat steps 1 through 10 using p = p(n) for the n + 1 iteration.

APPENDIX III
PROCEDURE FOR EVALUATING THE PLATE ALIGNMENT FACTOR

To evaluate the angle of attack, α (see sketch), from the measured plate (disk) pressure, p_w, the local conditions approaching the plate must be known, that is, M and p. These are known in the free stream of a test section using the calibrated Mach number and the stilling chamber pressure to derive the corresponding p. Or a reading from a surface tap on a model or tunnel wall combined with a pitot probe reading obtained at the same location as the plate will provide the local (Rayleigh) Mach number, M. It is required, of course, that there be no static pressure variation between this surface and the probe.

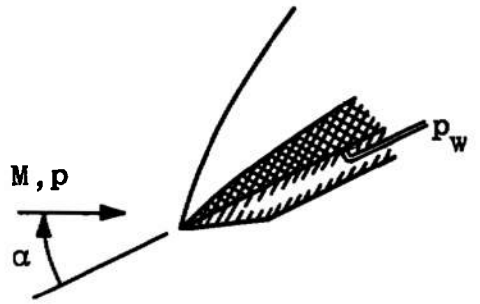

This strictly requires an iteration procedure which is initiated assuming that the ratio of inviscid pressure on the plate (p_{iw}) to the local pressure (p) is equal to p_w/p.

1. Compute the inviscid plate Mach number.

$$M'_{iw} = \sqrt{\frac{M^2 - 5\left[1 - (p_{iw}/p)^{2/7}\right]}{(p_{iw}/p)^{2/7}}}$$

2. Compute the inviscid plate length Reynolds number parameter.

$$(Re_\ell/C)_{iw} = (Re_\ell/C)(p_{iw}/p)(M_{iw}/M)(T/T_{iw})^{1.5}$$

where

$$(Re_\ell/C) = \frac{0.343 \ell p M (T_w/T)}{\mu_w T^{0.5}}, \text{ a constant}$$

$$T_w = T(1 + 0.173M^2)$$

$$T = T_t \div (1 + 0.2M^2)$$

$\mu_w \doteq \mu(T_w)$, see Appendix II, Step 5.

3. Compute the plate viscous interaction parameter.

$$\bar{X}_{iw} = M_{iw}^3 \div \sqrt{(Re_\ell/C)_{iw}}$$

4. Calculate the plate viscous interaction.

$$\frac{p_w}{p_{iw}} = 1 + A\bar{X}_{iw}$$

where A = 0.45 (Ref. 21, p. 344).

5. Compute the effect of plate angle of attack on the pressure ratio.

$$\frac{p_{iw}}{p} = \frac{(p_w/p)}{p_w/p_{iw}}$$

6. Compute the relative change in (p_{iw}/p) from Step 5 with that used in Step 1 to check for convergence to acceptable answer.

$$\left| \frac{(p_{iw}/p)_n - (p_{iw}/p)_{n-1}}{(p_{iw}/p)_{n-1}} \right| = R$$

If $R \leq 0.001$, go to Step 7, but if $R > 0.001$, go to Step 1.

7. Compute the alignment factor, K_α, and the plate angle of attack, α, based on thin-airfoil theory (Ref. 21, p. 109).

$$K_\alpha = (p_{iw}/p - 1)(M^2 - 1)^{1/2}/M^2 \qquad \text{for } M > 1$$

and

$$\alpha = 40.9\, K_\alpha$$

UNCLASSIFIED

Security Classification

DOCUMENT CONTROL DATA - R & D

(Security classification of title, body of abstract and indexing annotation must be entered when the overall report is classified)

1 ORIGINATING ACTIVITY (Corporate author) Arnold Engineering Development Center Arnold Air Force Station, Tennessee 37389	2a. REPORT SECURITY CLASSIFICATION UNCLASSIFIED 2b. GROUP N/A

3 REPORT TITLE

EVALUATION OF PROBES FOR MEASURING STATIC PRESSURE IN SUPERSONIC AND HYPERSONIC FLOWS

4 DESCRIPTIVE NOTES (Type of report and inclusive dates)

Final Report - July to October 1970

5. AUTHOR(S) (First name, middle initial, last name)

J. Don Gray, ARO, Inc.

6. REPORT DATE	7a. TOTAL NO OF PAGES	7b. NO. OF REFS
January 1972	42	21

8a. CONTRACT OR GRANT NO.	9a. ORIGINATOR'S REPORT NUMBER(S)
b. PROJECT NO. 8219	AEDC-TR-71-265
c. Program Element 62201F	9b. OTHER REPORT NO(S) (Any other numbers that may be assigned this report)
d.	ARO-VKF-TR-71-212

10 DISTRIBUTION STATEMENT

Approved for public release; distribution unlimited.

11 SUPPLEMENTARY NOTES	12. SPONSORING MILITARY ACTIVITY
Available in DDC	AEDC, Arnold AFS, TN 37389

13. ABSTRACT

The pertinent facts in the literature have been examined regarding the aerodynamic characteristics of static-pressure measuring probes in order to assess the relative merits and limitations of cone-cylinder, sharp-cone, and planar (disk) probes. The effects of Mach number, angle of attack, orifice location, and Reynolds number on the inferred local pressures were all evaluated at Mach numbers up to 8. It is concluded that the planar probe and sharp-cone probe (if properly designed) are equally more accurate than the cone-cylinder probe at supersonic and hypersonic speeds. However, the cone-cylinder is judged to be superior for use at Mach numbers below 4. Details of a recommended procedure to correct for the effects of viscous interaction (all probes) and angle of attack (planar probes only) are included.

DD FORM 1 NOV 65 1473

UNCLASSIFIED

Security Classification

14. KEY WORDS	LINK A		LINK B		LINK C	
	ROLE	WT	ROLE	WT	ROLE	WT
pressure measurement						
airspeed indicators						
pitot tubes						
supersonic wind tunnels						
hypersonic wind tunnels						
disk (planar) probes						
cone probes						
cone-cylinder probes						
angle of attack						
correction procedures						